Geophys. J. Int. (2001) **145,** 631–646

Acoustic wave propagation in one-dimensional random media: the wave localization approach

Mirko van der Baan*

School of Earth Sciences, University of Leeds, Leeds, LS2 9JT, *UK. E-mail: mvdbaan@earth.leeds.ac.uk*

Accepted 2000 December 12. Received 2000 September 9; in original form 1999 September 29

SUMMARY

Multiple wave scattering in strongly heterogeneous media is a very complicated phenomenon. Although a statistical approach may yield a considerable simplification of the mathematics, no guarantee exists that the theoretically predicted and the observed quantities coincide. The solution of this problem is to use self-averaging quantities only.

A multiple scattering theory that makes use of such self-averaging quantities is the so-called wave localization theory. This theory allows one to study both numerically and theoretically the influence of the presence of heterogeneities on the frequency-dependent dispersion and apparent attenuation of a pulse traversing a random medium. I calculate the localization length (penetration depth), the inverse quality factor and both the group and phase velocities for several chaotic media described by different autocorrelation functions. Calculations are limited to 1-D acoustic media with constant density. However, media studied range from very smooth to fractal-like and incidence is not limited to be vertical. I then compare the theoretical results with estimates of the same quantities obtained from numerical simulations.

The following can be concluded. (1) Theoretical predictions and numerical simulations agree in nearly the whole frequency domain for angles of incidence $\leq 30^{\circ}$ and relative standard deviations of the fluctuations of the incompressibility ≤ 30 per cent. (2) An inspection of the inverse quality factor confirms that the apparent attenuation is strongest in the domain of Mie scattering except for fractal-like media. In such media, no particular ratio of the wavelength to the typical scale length of heterogeneities is preferred since no such typical scale length exists. Hence, the inverse quality factor is constant over a large frequency band. (3) The group and phase velocities obtained agree with the effective medium theory and the Kramers–Krönig relations. That is, both converge to the effective medium velocity and the geometric velocity in the low- and high-frequency domains respectively. However, for intermediate frequencies, the exact behaviour strongly depends on the type of medium. Differences are related mainly to the number of extrema and Airy phases.

Key words: attenuation, dispersion, inhomogeneous media, scattering, statistical methods, wave propagation.

1 INTRODUCTION

Much has already been written about wave scattering and in particular the influence of small- and large-scale heterogeneities on the dispersion and apparent attenuation of a wave front traversing a heterogeneous medium. Sato & Fehler (1998), for instance, gave a good overview of theoretical and practical developments of the last 20 years, albeit in a seismological context only.

Although the wave scattering problem is completely described by linear partial differential equations, non-linearities are introduced as the solutions depend in a non-linear way on the coefficients of the differential equations. These coefficients are naturally random in random media (Frisch 1968). Hence, for heterogeneous media, exact solutions can only be established in some rare and extremely simplified cases. However, most of

* Formerly at: Laboratoire de Géophysique Interne et Tectonophysique, University Joseph Fourier, BP 53, 38041 Grenoble Cedex 9, France.

these solutions are formulated in terms of infinite series, which do not always converge easily. Further complications arise due to the enormous number of variables that have to be dealt with, especially if a deterministic approach is chosen. Moreover, these mathematical complications make it very hard to improve our physical understanding of wave scattering in all its aspects.

One possible method to simplify the problem is to opt not for a deterministic but for a statistical approach. Whereas the first approach requires a full description of every single heterogeneity (magnitude, position, shape, orientation, etc.), in the latter approach media are completely described by their spatial autocorrelation functions, as these functions determine the characteristic magnitudes and scale lengths of the heterogeneities present and their respective roughnesses or smoothnesses. Such a statistical description is of particular interest if both the principal wavelength and the characteristic scale length of the heterogeneities are largely inferior to the dimensions of the random medium (or the path length considered). A sound mathematical review of the problem of wave propagation in random media can be found in Frisch (1968), whereas Herraiz & Espinosa (1987) and Sato & Fehler (1998) dealt with more practical issues.

Thus, the use of a statistical description of the random medium results in simplified mathematics and can, therefore, help to improve our understanding of the influence of heterogeneities on the dispersion and apparent attenuation of a wave front. Unfortunately, however, no guarantee exists that observed and theoretically predicted mean values coincide. That is, fluctuations may dominate in single realizations of the medium. Hence, the true mean can only be estimated if several configurations and thus independent measurements exist. This drawback makes statistical theories very hard to use for inversion purposes, especially if only a single realization exists, such as, for example, in the problem of wave propagation in the real Earth.

The solution to this problem is to use self-averaging quantities only. Such quantities assume their mean values in each single realization with unit probability provided that the wave passes through a sufficiently large medium, thereby endowing the mean values with the physical meaning of real observables (Gredeskul & Freĭlikher 1990; Shapiro & Zien 1993).

In this paper, I use the theory of wave localization, which deals with such self-averaging quantities only. In addition, this theory is particularly suited to strong scattering problems and therefore works well for large propagation distances (exceeding largely the mean free path) in contrast to other statistical approaches, which are described below.

The origin of the wave localization theory stems from the quantum theory of disordered solids and in particular from the seminal paper of Anderson (1958). In this discipline, it is now of mainstream interest [see, for example, the review articles of Ramakrishnan (1987), Souillard (1987) and Van Tiggelen (1999)]. However, the application of results developed in quantum mechanics to the theory of wave propagation in random media is of more recent origin. Interest in predictions of localization theory for multiple scattering of acoustic waves started only 25 years after the paper of Anderson (1958).

Wave localization implies that a wave has an exponential fall-off for large distances from its maximum, causing the envelope of a pulse to decrease exponentially for large propagation distances in 1-D random media. To put it another way, the transmission coefficient T behaves like $|T| = \lim_{L\to\infty} \exp(-\gamma L)$ (for almost any frequency and almost any realization of the medium), with γ the so-called Lyapunov exponent.

The mathematical proof of such an exponential decay comes from the discipline of random matrix theory. This discipline tries to predict asymptotic values for certain systems described by (transfer) matrix multiplications and can, therefore, be applied to wave propagation problems in 1-D media. Hence, random matrix theory can establish theoretical predictions for certain problems described by linear partial differential equations with random coefficients, such as some multiple scattering problems.

The principal theorems needed to prove the above statement are those of Fürstenberg (1963) and Oseledec (1968) for stationary and ergodic random media. Sometimes Virster (1979) theorem is also invoked, which yields a generalization of the first two theorems. Fürstenberg's theorem states that the Lyapunov exponent γ exists and is positive for almost any frequency and is non-random for almost any realization of the random medium. Oseledec's theorem, on the other hand, states that γ exists pairwise (Souillard 1987). That is, for 2×2 matrices there exist both a positive and a negative γ with equal absolute magnitudes. Hence, mathematically both an exponentially increasing and decreasing wave exist with unit probability. Although the physically non-realistic exponentially growing wave dominates for random boundary conditions, implementing the right boundary conditions (in particular, finite radiation conditions at $\pm$infinity) will eliminate it. Proofs can also be found in Lifshits *et al.* (1988). Delyon *et al.* (1983) gave a simplified proof holding for 2×2 matrices only.

The Lyapunov exponent γ almost certainly satisfies the above-mentioned statements (more general results cannot be obtained). Nevertheless, it is a self-averaging quantity, that is, it reaches its predicted value with unit probability for large distances as only a finite, i.e. countable, number of exceptions exist. One exception is related to the fact that for $f\to 0$ no wave scattering occurs, that is, in the long-wavelength limit the medium is effectively homogeneous and γ becomes zero as is shown later. Other exceptions are mainly related to the occurrence of resonances, e.g. due to periodic layering (Souillard 1987). Note, however, that the above theorems do imply that mean values may deviate from the theoretically predicted ones if they are dominated by atypical realizations. However, the probability for such an atypical realization to occur is zero.

In this paper, equations are derived for the dispersion and apparent attenuation of acoustic wave propagation in 1-D random media using first principles only and the above-described exponential decay of the transmission coefficient due to wave localization. First, the mathematical problem of wave propagation in chaotic media is formulated and some reasons are given to explain the different behaviour of quantum mechanical and classical wave localization. Then, it is shown that a medium becomes effectively homogeneous in the long-wavelength limit. Next, to obtain and analyse the frequency-dependent apparent attenuation and dispersion due to wave scattering, the second-order perturbation expansion of Shapiro & Zien (1993) is used. Finally, numerical simulations are performed to determine to what extent theoretical predictions and practice agree. Data is analysed using the wavelet transform, which produces considerably more accurate results using single realizations only than those obtained in other studies and numerical tests.

2 THEORY

2.1 Posing the problem: wave propagation through random media

In this paper, wave propagation in random media is considered. The chaotic background parameters of the media are described by statistical means using a standard deviation and a particular autocorrelation function. The standard deviation determines the characteristic magnitude and the autocorrelation function the typical scale length of the heterogeneities and the amount of smoothness or roughness present.

As a first physical insight is most easily obtained from a simplified approach, several assumptions are made to simplify the mathematics. Nevertheless, large parts of the full mathematical 1-D problem are already known and are referred to in due course. In addition, the influence of dropping these simplifications is briefly alluded to.

First, only acoustic wave propagation in perfect 1-D media without energy absorption (dissipation) is considered. Although I limit the analysis to 1-D media, non-vertical incidence is allowed for. Moreover, only acoustic waves are dealt with to prevent complications due to the co-existence of both P and S waves and their coupling. Second, fluctuations are assumed to be static and stationary. However, relative standard deviations of up to 30 per cent can be handled rather well by the theory. Such standard deviations are largely sufficient to account for most 1-D models. Finally, the medium is assumed to be ergodic.

Scales are all-determining in wave scattering problems. The two most important scales are ka and kL, with a the typical scale length of the heterogeneities, L the thickness of the random part of the medium and k the wavenumber ($k=2\pi/\lambda$, with λ the wavelength of the probing pulse). Wave localization occurs only if $kL \gg 1$ and $a \ll L$, which places some constraints on ka.

Fluctuations of the density $\rho(z)$ and incompressibility $\kappa(z)^{-1}$ profiles are described by

$$\begin{cases} \rho(z) = \rho_0[1 + \sigma_\rho(z)] \\ \kappa^{-1}(z) = \kappa_0^{-1}[1 + \sigma_\kappa(z)] \end{cases}, \tag{1}$$

where z is positive with depth. Thus, the fluctuations are superposed on a constant profile. The relative perturbations σ_ρ and σ_κ are assumed to be stationary and have an expectancy, i.e. average, of zero.

Furthermore, I distinguish between three scales, namely, a microscopic scale associated with random fluctuations, a macroscopic scale associated with propagation distances and finally the intermediate scale of the pulse width, which will be called the mesoscopic scale.

2.2 Quantum mechanical and classical waves

Localization is a phenomenon characteristic of waves in random media. It is well known that for (infinite) systems described by one or two spatial dimensions, both quantum mechanical and classical waves are localized if an infinitesimal amount of randomness is present for sufficiently large propagation distances. This phenomenon was first predicted by the scaling theory of localization (Abrahams *et al.* 1979). Although the basic physics of localization are common for both types of waves, specific behaviour is expected to differ due to different dispersion relations and boundary conditions. Examples of different behaviour can be found in wave propagation characteristics and in the frequency dependence of the localization length (Sheng *et al.* 1986). Physically, this can directly be deduced from the fact that quantum mechanical waves are described by the Schrödinger equation, whereas classical waves are best described by the Helmholtz equation.

To illustrate this fact, I use the 1-D classical wave equation for vertical incidence, i.e.

$$\partial_{zz}u(z, t) - \frac{1}{c^2(z)}\,\partial_{tt}u(z, t) = 0\,, \tag{2}$$

where ∂_{zz} stands for $\partial^2/\partial z^2$. Technically, this formulation implies constant κ, but this is not relevant for the present analysis.

Fourier transforming eq. (2) and decomposing the velocity as

$$\frac{1}{c^2(z)} = \frac{1}{c_0^2}\,(1 - V(z)) \tag{3}$$

results in

$$\partial_{zz}u(z, \omega) + k_0^2 u(z, \omega) = k_0^2 V(z) u(z, \omega)\,, \tag{4}$$

where the dispersion relation $k=\omega/c$ has been used. This decomposition has already been used by Snieder (1990) and Dorren & Snieder (1995) to demonstrate some other similarities and disimilarities between classical and quantum mechanical waves. It should be noted that $(1-V)$ not only represents the squared relative slowness perturbation, but may also be identified with either the dielectric constant or the squared index of refraction, two variables that are more frequently encountered in optics.

If we compare eq. (4) with the 1-D Schrödinger equation, we can see that the right-hand side in the classical wave equation is not constant but directly proportional to the wave energy k_0^2. This in contrast to the Schrödinger equation, given by

$$\partial_{zz}u(z, \omega) + Eu(z, \omega) = V(z)u(z, \omega)\,. \tag{5}$$

Hence, a quantum mechanical particle becomes more and more localized in disordered systems as its energy E decreases, since the potential $V(z)$ gains in importance. Thus, localization of quantum mechanical particles (e.g. electrons) is always possible in the low-frequency domain, since the energy of quantum particles is also proportional to frequency.

In contrast to this, in the low-frequency domain the influence of the potential barrier $V(z)$ decreases with frequency for classical waves. In fact, a low-frequency classical wave tends to perceive the disordered system as an essentially homogeneous medium. Thus, in the low-frequency domain, no localization exists for classical waves, which is shown hereafter using an approach leading to the effective medium theory of Backus (1962).

2.3 Effective medium theory: homogenization

To show that no localization exists in the low-frequency limit, a pulse propagating through the random medium is considered. However, the propagation distance is limited to several wavelengths. In fact, it is better to speak of the long-wavelength limit than the low-frequency limit, since it is the ratio L/λ that has to tend to zero (Sheng 1995).

To display the homogenization phenomenon, Burridge *et al.* (1994) used the wave equation formulated as

$$\begin{cases} \rho\partial_t\dot{w} + \partial_z p = 0 \\ \kappa^{-1}\partial_t p + \partial_z\dot{w} = 0 \end{cases}, \tag{6}$$

with $\dot{w}$ the vertical particle velocity, p the pressure and ∂_z and ∂_t the partial derivatives for depth and time, respectively. Using a small-perturbation expansion, they showed that the behaviour of a pulse propagating in the 1-D random medium eq. (1) at normal incidence is determined by

$$\begin{cases} \langle\rho\rangle\partial_t\dot{w} + \partial_z p = 0 \\ \langle\kappa^{-1}\rangle\partial_t p + \partial_z\dot{w} = 0 \end{cases}. \tag{7}$$

In addition, p and $\dot{w}$ are not sensitive to the microscopic perturbations. Hence, the shape of the pulse remains constant. This implies that probing pulses travel as if through a homogeneous medium for propagation distances of the order of a wavelength. This phenomenon is also known as the effective medium theory of Backus (1962).

Thus, any medium appears locally homogeneous, at least for propagation distances of the order of a wavelength. However, for larger distances, the pulse is attenuated and broadened due to multiple scattering. Nevertheless, the theory does imply that, in the long-wavelength limit, no localization of energy occurs, since the medium appears homogeneous to the pulse, which, therefore, remains constant in amplitude and shape.

Another interesting feature of the effective medium theory is that it shows how averaging has to be done. Namely, the local vertical velocity c_v is given by

$$c_v^2 = \langle\kappa^{-1}\rangle^{-1}\langle\rho\rangle^{-1}. \tag{8}$$

Thus, the local compressibility has to be calculated using the harmonic mean, whereas density is given by its arithmetic average to obtain the effective vertical velocity.

The more elaborate analysis of Asch *et al.* (1991) shows that the horizontal velocity c_h is given by

$$c_h^2 = \langle\kappa^{-1}\rangle^{-1}\langle\rho^{-1}\rangle, \tag{9}$$

thereby indicating the existence of anisotropy due to fine-scale layering—a fact also stated by Backus (1962).

Eqs (8) and (9) are very interesting as they teach us how the phase velocity at zero frequency for vertical incidence has to be evaluated. It follows that c_0, the effective velocity, is given by

$$c_0 \equiv \langle\rho_0/\kappa_0\rangle^{-1/2} = \langle c^{-2}\rangle^{-1/2}. \tag{10}$$

Its high-frequency equivalent, i.e. the geometric velocity, can be calculated by averaging traveltimes over layer thicknesses, i.e.

$$c_\infty = \langle c^{-1}\rangle^{-1}, \tag{11}$$

which results in

$$c_\infty \approx c_0\left[1 - \frac{1}{8}\langle\sigma_\kappa^2\rangle\right]^{-1} + O(\sigma_\kappa^3) \approx c_0\left[1 + \frac{1}{8}\langle\sigma_\kappa^2\rangle\right] + O(\sigma_\kappa^3) \tag{12}$$

for a constant-density profile and vertical incidence. Eq. (12) is most easily established using a second-order Taylor expansion of eq. (1) and remembering that $\langle\sigma_\kappa\rangle = 0$. However, it is only valid for small values of σ_κ, constant ρ_0 and κ_0 and stationary σ_κ.

It should be noted that the predicted homogenization and the effective medium theory of Backus (1962) hold true for any medium, be it periodic or chaotic, whereas wave localization can only occur in non-periodic media. The non-existence of wave localization for periodic media will be shown below.

2.4 Amplitude and phase: two self-averaging quantities

2.4.1 Amplitude

Localization in quantum mechanics implies that energy is bounded in a specific region of a disordered medium and has an exponential decay outside this region. As was already mentioned above, a similar phenomenon occurs if a classical wave enters a disordered medium. Namely, the energy of the probing pulse (and thus its amplitude) decays exponentially with penetration depth due to multiple wave scattering. Hence, the transmission coefficient decays as

$$|T| = \lim_{z\to\infty} e^{-\gamma z} \Leftrightarrow \gamma = \lim_{z\to\infty} -\frac{1}{z}\ln|T|, \tag{13}$$

where γ is known as the Lyapunov exponent and depends on both frequency and the characteristics of a medium. The reciprocal γ^{-1} of the Lyapunov exponent is equivalent to the (maximum) localization length $l(f)$ and defines the characteristic attenuation length or penetration depth of a specific medium. The definition for amplitude decay has been used here.

To obtain an expression for $l(f)$, Shapiro & Zien (1993) considered a so-called matched medium, that is, the chaotic medium (eq. 1) has a thickness L and is sandwiched between two homogeneous half-spaces with matching density and compressibility. Moreover, it is assumed that ρ_0 and κ_0^{-1} are constant and σ_κ stationary. In addition, as a further simplification, the density is assumed to be constant in the whole medium, i.e. $\sigma_{\rho=0}$. Thus, the random medium is described by

$$\begin{aligned} \kappa^{-1}(z) &= \begin{cases} \kappa_0^{-1}, & z < 0,\ z > L \\ \kappa_0^{-1}[1 + \sigma_\kappa(z)], & 0 \le z \le L \end{cases}, \\ \rho(z) &= \rho_0 \qquad \text{everywhere}. \end{aligned} \tag{14}$$

To determine the behaviour of a wave propagating in such a system, they considered a plane wave impinging from above on the inhomogeneous layer. Using a second-order perturbation of the resulting wave equation and by assuming that σ_κ is stationary and has zero mean, it can be shown that the localization length is determined by

$$\begin{aligned} l^{-1} &= \frac{k_0^2}{4\cos^2(\phi_i)}\int_0^\infty \mathrm{E}[\sigma_\kappa(z)\sigma_\kappa(z+\xi)]\cos(2k_0\cos(\phi_i)\xi)d\xi \\ &= \frac{k_0^2}{8\cos^2(\phi_i)}\int_{-\infty}^\infty \mathrm{E}[\sigma_\kappa(z)\sigma_\kappa(z+\xi)]\,e^{-2ik_0\cos(\phi_i)\xi}d\xi \end{aligned} \tag{15}$$

if the higher moments of σ_κ decrease sufficiently fast (Shapiro & Zien 1993). A detailed derivation can be found in Shapiro & Hubral (1999). $\mathrm{E}[\sigma_\kappa(z)\sigma_\kappa(z+\xi)]$ represents the spatial autocorrelation function of the random medium. Moreover, eq. (15) leads to the well-known O'Doherty–Anstey relation. Thus, their relation can be understood as a wave localization phenomenon (Shapiro & Zien 1993).

2.4.2 *Phase*

Lifshits *et al.* (1988) proved that the Lyapunov exponent is not the only self-averaging quantity. The phase of the pulse divided by L is also self-averaging (as it represents the imaginary part of the signal and the pulse has to remain causal). Hence, the second self-averaging quantity ψ is defined by

$$\psi = \lim_{L\to\infty} \frac{\vartheta_s(L)}{L}\,. \tag{16}$$

A similar derivation as for the Lyapunov coefficient γ yields (Shapiro *et al.* 1994; Shapiro & Hubral 1999)

$$\psi = k_0\cos(\phi_i) - \frac{k_0^2}{4\cos^2(\phi_i)}\int_0^\infty \mathrm{E}[\sigma_\kappa(z)\sigma_\kappa(z+\xi)] \times \sin(2k_0\cos(\phi_i)\xi)d\xi\,. \tag{17}$$

Note that ψL represents the unwrapped phase. Therefore, ψ equals the effective vertical wavenumber.

2.4.3 *Ergodicity*

In geophysical or seismological applications only a single realization of the Earth exists. Therefore, ergodicity has to be invoked, that is, ensemble (or configurational) averaging can be replaced by spatial averaging:

$$\mathrm{E}[\sigma_\kappa(z)\sigma_\kappa(z+\xi)] = \langle\sigma_\kappa(z)\sigma_\kappa(z+\xi)\rangle \equiv \lim_{z\to\infty}\frac{1}{z}\int_0^z \sigma_\kappa(z')\sigma_\kappa(z'+\xi)dz'\,, \tag{18}$$

with E[.] again the autocorrelation function of the medium.

2.5 Frequency-dependent scattering and dispersion

To determine the behaviour of a pulse probing a chaotic medium and thereby the influence of small-scale heterogeneities on the frequency-dependent apparent attenuation and dispersion, three different spatial autocorrelation functions are considered. These are the Gaussian, exponential and Von Kármán correlation functions. Gaussian correlation functions are related to very smooth media (they are infinitely differentiable), whereas exponential autocorrelation functions are only piecewise continuous and contain, therefore, first-order discontinuities. The Von Kármán function (Tatarskii 1961), on the other hand, describes a very large class of correlation functions ranging from functions smoother than the exponential function to functions having discontinuities on all scales and therefore displaying fractal characteristics.

To analyse the phenomenon of multiple scattering, the frequency-dependent self-averaged amplitude, phase and the exact attenuation and vertical wavenumber are estimated. However, since the quality factor Q, the phase velocity c and the group velocity U are more commonly used in seismology, I also provide these. The scattering coefficient Q^{-1} is related to the Lyapunov exponent by

$$Q^{-1} = \frac{2\gamma}{k_0\cos(\phi_i)} \tag{19}$$

and the vertical phase velocity c_z is given by

$$c_z(f) = 2\pi f\psi^{-1} = \frac{c_0}{\cos(\phi_i)}\{1+\delta c\}\,, \tag{20}$$

where δc represents the relative perturbation of the phase velocity. The vertical group velocity U_z is associated with the actual propagation velocity of energy and can be calculated from

$$U_z(f) = \left[\frac{\partial\psi}{\partial\omega}\right]^{-1} = \frac{c_0}{\cos(\phi_i)}\{1+\delta U\}\,, \tag{21}$$

with δU the frequency-dependent part of the group velocity.

To simplify expressions, let k_0' denote $k_0\cos(\phi_i)$, the wavenumber corrected for the angle of incidence. All expressions are easily translated to the frequency domain using the dispersion relation, i.e. $k_0 = 2\pi f/c_0$.

2.5.1 *Gaussian correlation function*

If smooth transitions are assumed then the medium is best described using a Gaussian correlation function, i.e.

$$\mathrm{E}[\sigma_\kappa(z)\sigma_\kappa(z+\xi)] = \langle\sigma_\kappa^2\rangle\,\mathrm{e}^{-\xi^2/a^2}\,. \tag{22}$$

Substitution of this equation into eqs (15) and (17) yields

$$l_\mathrm{G} = \frac{8\cos^4(\phi_i)a}{\pi^{1/2}\langle\sigma_\kappa^2\rangle}(k_0'a)^{-2}\,\mathrm{e}^{(k_0'a)^2} \tag{23}$$

for the localization length and

$$\psi_\mathrm{G} = k_0'\left[1 - \frac{(k_0'a)^2\langle\sigma_\kappa^2\rangle}{4\cos^4(\phi_i)}\,{}_1F_1\left(1;\,1.5;\,-(k_0'a)^2\right)\right] \tag{24}$$

for the self-averaged phase. Expression (24) is obtained using the table of integrals of Gradshteyn & Ryzhik (1980). ${}_1F_1(.)$ represents the degenerate or confluent hypergeometric function. Furthermore, the inverse quality factor Q^{-1} is expressed (using eqs 19 and 23) by

$$Q_\mathrm{G}^{-1} = \frac{\pi^{1/2}\langle\sigma_\kappa^2\rangle}{4\cos^4(\phi_i)}\,k_0'a\,\mathrm{e}^{-(k_0'a)^2}\,. \tag{25}$$

The frequency-dependent part of the dispersion, i.e. δc in expression (20), is

$$\delta c_\mathrm{G} \approx \frac{(k_0'a)^2\langle\sigma_\kappa^2\rangle}{4\cos^4(\phi_i)}\,{}_1F_1\left(1;\,1.5;\,-(k_0'a)^2\right) + O(\sigma_\kappa^4)\,. \tag{26}$$

Finally, using eqs (21) and (24) and the relation

$$\frac{d\,{}_1F_1(\alpha;\gamma;z)}{dz} = \frac{\alpha}{\gamma}\,{}_1F_1(\alpha+1;\gamma+1;z) \tag{27}$$

(Gradshteyn & Ryzhik 1980), the vertical group velocity is established to be

$$U_{\mathrm{G},z} = \frac{c_0}{\cos(\phi_i)}\left[1 - \frac{3}{4}\frac{\langle\sigma_\kappa^2\rangle}{\cos^4(\phi_i)}(k_0'a)^2\,{}_1F_1(1;\,1.5;\,-(k_0'a)^2) + \frac{1}{3}\frac{\langle\sigma_\kappa^2\rangle}{\cos^4(\phi_i)}(k_0'a)^4\,{}_1F_1(2;\,2.5;\,-(k_0'a)^2)\right]^{-1}. \tag{28}$$

Hence, δU_G is

$$\delta U_G \approx \frac{3}{4}\frac{\langle\sigma_\kappa^2\rangle}{\cos^4(\phi_i)}(k_0'a)^2\,{}_1F_1\left(1;\,1.5;\,-(k_0'a)^2\right)$$

$$-\frac{1}{3}\frac{\langle\sigma_\kappa^2\rangle}{\cos^4(\phi_i)}(k_0'a)^4\,{}_1F_1(2;\,2.5;\,-(k_0'a)^2)+O(\sigma_\kappa^4)\,. \quad (29)$$

Analysis of eqs (23)–(29) for all frequencies teaches us the following (see also Fig. 1).

(i) The localization length behaves as $l_G \sim k_0^{-2}$ in the low-frequency domain and as $l_G \to \infty$ for very high frequencies. Hence, no localization of energy exists in either limit. Physically, this is due to the fact that in the low-frequency domain (long-wavelength limit) the medium becomes effectively homogeneous. No scattering occurs in the high-frequency limit either, since no discontinuities are present in smooth media in that limit. The f^2 dependence of l_G^{-1} is explained by the f^2 frequency variation of Rayleigh scattering for stratified media or generally f^{d+1} for d-dimensional media (White *et al.* 1990). Finally, a minimum localization length exists for $k_0'a=1$ or $\lambda = 2\pi a$ for vertical incidence, thereby favouring Mie scattering.

(ii) The scattering coefficient Q_G^{-1} displays a similar behaviour. No scattering occurs in either the low- or high-frequency limit. Furthermore, a maximum in the apparent attenuation due to scattering occurs for $k_0'a = \sqrt{2}/2$, yielding again the fact that scattering is most efficient for wavelengths of the same order as the correlation length of the heterogeneities, i.e. due to Mie scattering.

(iii) The vertical wavenumber ψ_G behaves as

$$\lim_{k_0\to 0}\psi_G = k_0' \quad (30)$$

in the low-frequency limit and as

$$\lim_{k_0\to\infty}\psi_G = k_0'\left[1-\frac{\langle\sigma_\kappa^2\rangle}{8\cos^4(\phi_i)}\right] \quad (31)$$

in the high-frequency limit. This last expression can be found using the relation (Abramowitz & Stegun 1972)

$${}_1F_1(a;\,b;\,z)$$

$$=\frac{\Gamma(b)}{\Gamma(b-a)}(-z)^{-a}\left[1+O\left(|z|^{-1}\right)\right],\ |z|\to\infty \text{ and } z<0\,, \quad (32)$$

where $\Gamma(.)$ represents the Gamma function. Eq. (30) clearly shows the occurrence of the homogenization phenomenon in the low-frequency domain. Using eq. (20), we obtain for δc_G in the high-frequency limit

$$\lim_{k_0\to\infty}\delta c_G = \frac{\langle\sigma_\kappa^2\rangle}{8\cos^4(\phi_i)} \quad (33)$$

if higher-order moments of σ_κ are neglected. Eqs (30) and (31) or (33) confirm eqs (10) and (12) for constant-density profiles and vertical incidence. Thus, the phase velocity satisfies the established values for both the effective (c_0) and the geometric (c_∞) velocities. Finally, the phase velocity shows an overshoot with a maximum at approximately $k_0'a=1.5$ (Fig. 1).

(iv) The group velocity also satisfies the established values for the effective (c_0) and geometric (c_∞) velocities. Moreover, Airy phases (i.e. extrema of the group velocity curve) occur at $k_0'a=0$, 0.96 and 2.18 and for $k_0'a\to\infty$. Airy phases are normally associated with strong arrivals as waves are allowed

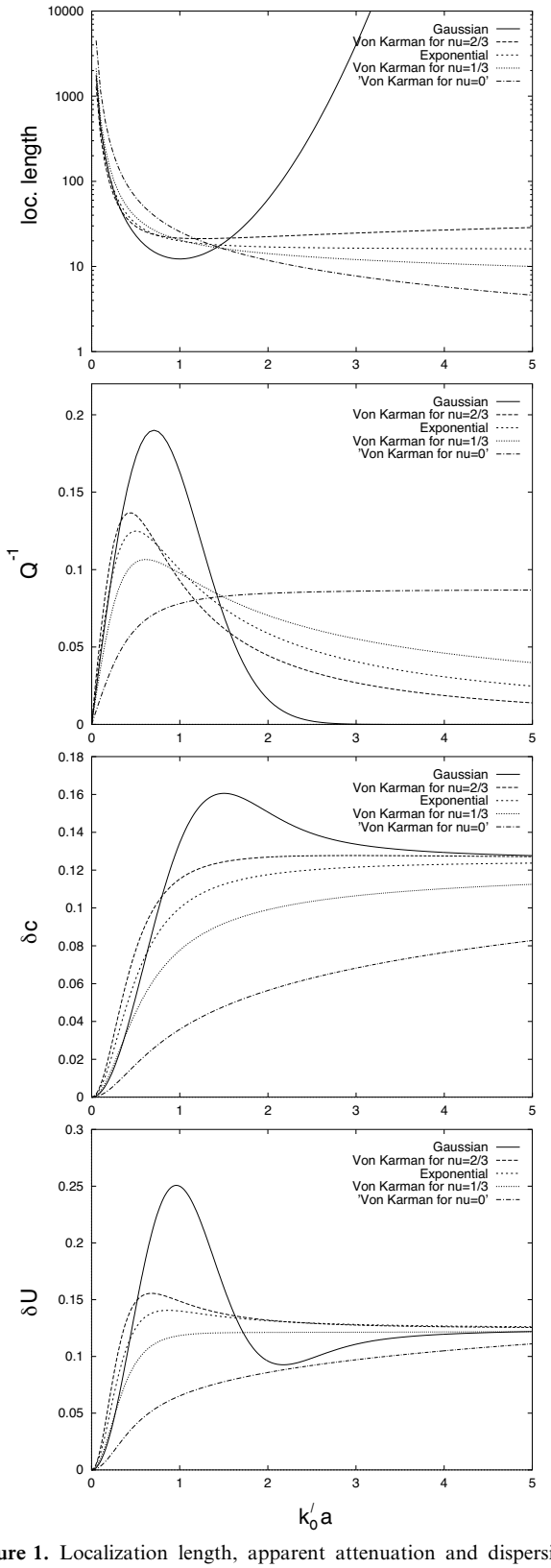

Figure 1. Localization length, apparent attenuation and dispersion as a function of $k_0'a$. Vertical scales have been normalized with $\langle\sigma_\kappa^2\rangle/\cos^4(\phi_i)$. In addition, units of the localization length are expressed in typical scale lengths a. The constant $\Gamma(0)$ in the Von Kármán function for $\nu=0$ has been replaced by the constant 9.0 to display the general trend. Notice the strong dependence of all quantities on the angle of incidence, indicating, for example, the presence of anisotropy due to fine-scale layering.

to interfere constructively over a large frequency band due to the presence of an extremum (because of the absence of dispersion). Naturally, Airy phases occur in both frequency limits, since no dispersion exists in these extremes. However, the second Airy phase is situated in the Mie scattering domain, rendering it hard to detect. Nevertheless, the third one may be detectable as it is characterized by a very high quality factor (Fig. 1).

2.5.2 *Exponential correlation function*

If an exponential spatial correlation between heterogeneities exists then the ensemble averaging can be replaced by

$$\mathrm{E}[\sigma_\kappa(z)\sigma_\kappa(z+\xi)] = \langle\sigma_\kappa^2\rangle\, \mathrm{e}^{-|\xi|/a}. \tag{34}$$

Thus, substitution of this equation into eqs (15) and (17) yields

$$l_{\mathrm{exp}} = \frac{4\cos^4(\phi_i)a}{\langle\sigma_\kappa^2\rangle}\left[4 + (k_0'a)^{-2}\right]$$

$$= \frac{16\cos^4(\phi_i)a}{\langle\sigma_\kappa^2\rangle} + \frac{c_0^2\cos^2(\phi_i)}{\pi^2\langle\sigma_\kappa^2\rangle a} f^{-2}, \tag{35}$$

$$\psi_{\mathrm{exp}} = k_0'\left[1 - \frac{\langle\sigma_\kappa^2\rangle}{2\cos^4(\phi_i)}\frac{(k_0'a)^2}{4(k_0'a)^2+1}\right] \tag{36}$$

and for the apparent attenuation due to scattering (using eq. 19)

$$Q_{\mathrm{exp}}^{-1} = \frac{\langle\sigma_\kappa^2\rangle}{2\cos^4(\phi_i)}\frac{k_0'a}{4(k_0'a)^2+1}. \tag{37}$$

Moreover, δc_{exp} can be found to be

$$\delta c_{\mathrm{exp}} \approx \frac{\langle\sigma_\kappa^2\rangle}{2\cos^4(\phi_i)}\frac{(k_0'a)^2}{4(k_0'a)^2+1} + O(\sigma_\kappa^4) \tag{38}$$

using expression (20). Finally, we find for the vertical group velocity $U_{\mathrm{exp},z}$ (with eqs 21 and 36)

$$U_{\mathrm{exp},z} = \frac{c_0}{\cos(\phi_i)}\left[1 - \frac{\langle\sigma_\kappa^2\rangle}{2\cos^4(\phi_i)}\frac{(k_0'a)^2(4(k_0'a)^2+3)}{(4(k_0'a)^2+1)^2}\right]^{-1} \tag{39}$$

and for δU_{exp}

$$\delta U_{\mathrm{exp}} \approx \frac{1}{2}\frac{\langle\sigma_\kappa^2\rangle}{\cos^4(\phi_i)}\frac{(k_0'a)^2(4(k_0'a)^2+3)}{(4(k_0'a)^2+1)^2} + O(\sigma_\kappa^4). \tag{40}$$

Analysis of eqs (35)–(40) teaches us the following (see also Fig. 1).

(i) The localization length l_{exp} behaves again as $l_{\mathrm{exp}} \sim f^{-2}$ in the low-frequency domain. However, it saturates to a constant for $f \to \infty$, since exponential models are associated with piecewise continuous media. Hence, above a certain frequency, all wavelengths will 'sense' all discontinuities in exactly the same way.

(ii) The scattering coefficient Q_{exp}^{-1} shows a different behaviour from l_{exp}. It is more similar to Q_{G}^{-1} as Q_{exp}^{-1} goes to zero for either frequency limit. Moreover, the apparent attenuation is maximal for $k_0a = 1/2$, thereby again favouring Mie scattering.

(iii) The effective vertical wavenumber ψ_{exp} shows a similar behaviour to ψ_{G} in both frequency limits, that is, an effective homogeneous medium for $k_0 \to 0$ given by expression (30) and a speed up of velocity for $k_0 \to \infty$ given by expressions (31) and (33). However, δc_{exp} is monotonically rising (Fig. 1).

(iv) The group velocity again satisfies both velocity limits. However, now only three Airy phases exist as usual in the low- and high-frequency limits and for $k_0'a = \sqrt{3}/2$. Strangely, the second Airy phase occurs again in the domain of Mie scattering. Hence, it cannot be associated with a strong arrival.

2.5.3 *Von Kármán correlation function*

The third kind of correlation function to be examined is the Von Kármán function, which describes a very large class of models, ranging from smooth media to fractal-like models. It is given by

$$\mathrm{E}[\sigma_\kappa(z)\sigma_\kappa(z+\xi)] = \frac{2^{1-\nu}\langle\sigma_\kappa^2\rangle}{\Gamma(\nu)}\left(\frac{|\xi|}{a}\right)^\nu K_\nu\left(\frac{|\xi|}{a}\right), \tag{41}$$

where $K_\nu(.)$ represents the third modified Bessel function of order ν, also known as the MacDonald function. Autocorrelation functions described by it include the Kolmogorov turbulence function ($\nu = 1/3$), the exponential correlation function ($\nu = 1/2$) and a function with fractal characteristics ($\nu = 0$) having discontinuities on any scale. In general, ν is limited to range between 0 and 1. For $\nu > 1/2$, functions are smoother than the exponential function and rougher for $\nu < 1/2$. In eq. 41, $K_0(0)$ is defined as $\Gamma(0)/2$ to produce a value equal to the variance for zero lag ($\xi = 0$). The solutions to the integrals of eqs (15) and (17) with a Von Kármán correlation function can be found using the table of integrals of Gradshteyn & Ryzhik (1980), resulting in

$$l_{\mathrm{VK}} = \frac{4\cos^4(\phi_i)a\Gamma(\nu)}{\langle\sigma_\kappa^2\rangle\sqrt{\pi}\Gamma(\nu+1/2)}\frac{(4(k_0'a)^2+1)^{\nu+1/2}}{(k_0'a)^2} \tag{42}$$

for $a^{-1} > 0$, $k_0 > 0$ and $\nu > -1/2$ and for ψ_{VK} in

$$\psi_{\mathrm{VK}} = k_0'\left[1 - \frac{\langle\sigma_\kappa^2\rangle\Gamma(\nu+1)}{\cos^4(\phi_i)\Gamma(\nu)}(k_0'a)^2 \times {}_2F_1\left(\nu+1,\, 1;\, 1.5;\, -4(k_0'a)^2\right)\right] \tag{43}$$

for $\nu > -1$. Note that $\Gamma(\nu+1)/\Gamma(\nu)$ may be replaced by ν for $\nu \neq 0$. The function ${}_2F_1(.)$ is known as Gauss' hypergeometric function. Furthermore, the apparent attenuation due to scattering is given by

$$Q_{\mathrm{VK}}^{-1} = \frac{\langle\sigma_\kappa^2\rangle\sqrt{\pi}\Gamma(\nu+1/2)}{2\cos^4(\phi_i)\Gamma(\nu)}\frac{k_0'a}{(4(k_0'a)^2+1)^{\nu+1/2}} \tag{44}$$

and δc_{VK} by

$$\delta c_{\mathrm{VK}} \approx \frac{\langle\sigma_\kappa^2\rangle\Gamma(\nu+1)}{\cos^4(\phi_i)\Gamma(\nu)}(k_0'a)^2 \times {}_2F_1\left(\nu+1,\, 1;\, 1.5;\, -4(k_0'a)^2\right) + O(\sigma_\kappa^4). \tag{45}$$

Finally, the group velocity can be calculated using eqs (21) and (43) and the relation

$$\frac{d_2F_1(a,b;c;z)}{dz} = \frac{ab}{c}\,{}_2F_1(a+1, b+1; c+1; z) \tag{46}$$

(Abramowitz & Stegun 1972). This results in

$$U_{\mathrm{VK},z} = \frac{c_0}{\cos(\phi_i)}\left[1 - \frac{3\langle\sigma_\kappa^2\rangle\Gamma(\nu+1)}{\cos^4(\phi_i)\Gamma(\nu)}(k_0'a)^2 \times {}_2F_1\left(\nu+1, 1; 1.5; -(k_0'a)^2\right) + \frac{16(\nu+1)\langle\sigma_\kappa^2\rangle\Gamma(\nu+1)}{3\cos^4(\phi_i)\Gamma(\nu)}(k_0'a)^4 \times {}_2F_1\left(\nu+2, 2; 2.5; -(k_0'a)^2\right)\right]^{-1} \quad (47)$$

and

$$\delta U_{\mathrm{VK}} \approx \frac{3\langle\sigma_\kappa^2\rangle\Gamma(\nu+1)}{\cos^4(\phi_i)\Gamma(\nu)}(k_0'a)^2 \times {}_2F_1\left(\nu+1, 1; 1.5; -(k_0'a)^2\right) - \frac{16(\nu+1)\langle\sigma_\kappa^2\rangle\Gamma(\nu+1)}{3\cos^4(\phi_i)\Gamma(\nu)}(k_0'a)^4 \times {}_2F_1\left(\nu+2, 2; 2.5; -(k_0'a)^2\right) + O(\sigma_\kappa^4)\,. \quad (48)$$

Expressions (42)–(48) are more difficult to analyse than their equivalents for Gaussian or exponential correlation functions. Nevertheless, the following can be concluded (see also Fig. 1).

(i) The localization length is always proportional to f^{-2} in the low-frequency domain due to Rayleigh scattering. However, in the high-frequency domain, $l \sim f^{2\nu-1}$, implying a divergence for $\nu > 1/2$ (smooth models), the convergence to a constant for $\nu = 1/2$ (as it equals the exponential case) and a convergence to zero for $\nu < 1/2$. This last feature is due to the existence of discontinuities on any scale for $\nu < 1/2$. Therefore, no energy penetrates in the high-frequency limit for these values of ν. Thus, the statement of Sheng *et al.* (1986) that a minimum localization length exists is not necessarily true for media displaying fractal-like characteristics.

(ii) The scattering coefficient Q^{-1} always equals 0 for $f \to 0$ due to the homogenization of the medium. Furthermore, in the high-frequency limit, Q^{-1} is proportional to $f^{-2\nu}$, implying again a convergence to zero for any ν except $\nu = 0$. Moreover, a maximum is present (except for $\nu = 0$). Such maxima occur always in the domain of Mie scattering, i.e. $k_0'a \approx 1$. However, they tend to shift to lower values of $k_0'a$ for increasing ν. On the other hand, for $\nu = 0$, Q^{-1} is monotonically rising and converges to a constant, i.e.

$$\lim_{f\to\infty} Q^{-1}_{\mathrm{VK},\nu=0} = \frac{\langle\sigma_\kappa^2\rangle\pi}{4\cos^4(\phi_i)\Gamma(0)}\,, \quad (49)$$

which is effectively zero due to the division by $\Gamma(0)$. A nearly constant Q^{-1} over a large frequency range may be characteristic of fractal-like distributions as fractals are self-affine. Hence, any scale length may be considered to be a typical dimension and Mie scattering will therefore occur everywhere.

(iii) Expression (43) is difficult to analyse analytically due to the presence of the hypergeometric function. Nevertheless, numerical calculations agree with previously obtained results, that is, limits (30) and (31) are satisfied for any ν ($0 \le \nu < 1$). Moreover, the smoother models ($\nu > 1/2$) tend to show an 'overshoot' (although this is not visible on the scale of Fig. 1), whereas rougher models ($\nu < 1/2$) are monotonically rising. Nevertheless, the limit (33) for δc is always satisfied in the high-frequency domain.

(iv) Numerical calculations of δU_{VK} reveal the following picture. Like the phase velocity, the group velocity satisfies both the limits for the effective and the geometric velocities. However, in between these limits, the exact behaviour depends strongly on the value of ν. For $\nu < 1/3$, δU is monotonically rising, for $1/3 < \nu < 0.40$ a transition zone occurs in which a maximum (overshoot) is followed by a minimum (analogous to the Gaussian case), for $0.40 < \nu < 1/2$ only the overshoot remains and for $\nu > 1/2$ the overshoot is again followed by a minimum (not visible on the scale of Fig. 1). Bounds have only been established approximately. As a consequence, the number and positions of Airy phases depends strongly on the exact value of ν. Nevertheless, a comparison of the established curves for Q^{-1} and δU in Fig. 1 clearly shows the existence of some direct relation between these two parameters. For instance, the maxima (or corners) in Q^{-1} and δU seem to be separated by a constant shift and both move to higher values of $k_0'a$ for decreasing ν.

A final note concerning the particular case of $\nu = 0$ is that the factor $\Gamma(0)$ is needed to normalize the Von Kármán function. However, in non-perfect realizations (e.g. due to finite layer thicknesses) it can be replaced by a constant that is much smaller than infinity. Nevertheless, its localization length seems to be much larger and c and U approach the geometric velocity for much higher frequencies than for the other autocorrelation functions.

2.5.4 *Kramers–Krönig relations*

A recent controversy has arisen concerning wave localization theory in that estimates of the effective (c_0) and the geometric (c_∞) velocities calculated from sonic well logs do not coincide with those derived from measurements of the localization length obtained by means of numerical wave propagation in these same well logs and the Kramers–Krönig relations. This might indicate a discrepancy between effective medium theory and wave localization theory (Scales 1993).

Nevertheless, both theories should give the same values for c_0 and c_∞ as for linear, passive and causal systems, $l^{-1}(f)$ and $c(f)$ are not independent of each other, but related by Hilbert transforms (Beltzer 1988). These relations are known as the Kramers–Krönig relations. For instance, c_0 and c_∞ are related to $l(f)$ by

$$c_\infty = c_0\left[1 - \frac{c_0}{\pi^2}\int_0^\infty \frac{df}{l(f)f^2}\right]^{-1} \quad (50)$$

(Beltzer 1988). I will show that this discrepancy is not due to a lack in theory, but does constitute an important issue for practical inversion problems.

White *et al.* (1990) were the first to try to estimate the frequency-dependent localization length in realistic numerical simulations using real sonic well log data as random models. They calculated the transmission coefficient $|T|$ of a synthetic wave passing through a single stack of layers, that is, without using configurational averaging. Scales (1993) showed, however, that their estimates of $l(f)$ were in contradiction to effective medium theory. The two limits of the dispersion curve, c_0 and c_∞, given by eqs (10) and (11) directly applied on the

sonic well logs were not identical to those implied by the estimated $l(f)$ and the Kramers–Krönig relations, thereby violating causality. Errors in the estimation of $l(f)$ were attributed by Scales (1993) to a possible lack of low-frequency information in seismic data.

If the wave localization theory satisfies the Kramers–Krönig relations, then relations between c_0 and c_∞ as predicted by eq. (50) should correspond independently to (i) expressions (30), (31) and (33) for the effective wavenumber in these limits and (ii) eqs (10) and (12) given by the effective medium theory. It has already been shown that eqs (30), (31) and (33) do confirm eqs (10) and (12) for Gaussian, exponential and Von Kármán autocorrelation functions. Moreover, inserting eqs (23) and (35) into expression (50) and performing the integration yields for the first two cases

$$c_\infty = c_0 \left[1 - \frac{1}{8} \langle \sigma_\kappa^2 \rangle \right]^{-1} \tag{51}$$

for vertical incidence. Thus, at least for exponential and Gaussian random media, wave localization theory in combination with the Kramers–Krönig relations and effective medium theory does yield the same limits for the dispersion curve up to second order. Unfortunately, again, no explicit analytical results could be obtained for the Von Kármán function, since integral (50) could not be solved. Nevertheless, this does indicate that the overshoot in the relative dispersion curve for Gaussian media (Fig. 1) is required for the traversing pulse to remain causal.

2.5.5 *Absence of localization*

In the Introduction, it was mentioned that no wave localization occurs for a finite number of frequencies and a set of realizations with zero probability, which are mainly related to periodic layering and the occurrence of resonances. Before showing that the equations obtained for the localization length, i.e. eqs (23), (35) and (42), are in agreement with this statement, let us first note that the localization length is inversely proportional to the variance of the characteristic magnitude of the heterogeneities. This indicates that naturally no localization of energy can occur in the absence of heterogeneities. However, it also indicates that an infinitesimally small amount of randomness suffices to cause wave localization in 1-D media, which is in agreement with the scaling theory of localization of Abrahams *et al.* (1979).

Besides depending on the amount of randomness present, the localization length also directly depends on the ratio $k_0'a$ and on the characteristic scale length a of the heterogeneities itself. These two variables must be treated as two independent quantities and can be analysed separately. However, for fixed a, the ratio $k_0'a$ depends only on the frequency f or wavelength considered. Let us first examine the influence of $k_0'a$ and f on the localization length.

It was shown that independent of the type of correlation function used, i.e. Gaussian, exponential or Von Kármán, no wave localization occurs in the low-frequency domain (long-wavelength limit). This is due to the occurrence of Rayleigh scattering and the homogenization of the medium in this limit. Moreover, for smooth models, that is, for Gaussian and Von Kármán functions with $\nu > 1/2$, no localization occurs for high frequencies either (geometric limit), since no discontinuities are present for smooth models in this limit. Therefore, for the three types of autocorrelation functions used, only two frequencies form an exception to the statement that wave localization always occurs in 1-D media if an infinitesimally small amount of randomness is present.

The typical scale length a of the heterogeneities also influences the localization length. No localization occurs if a tends to infinity either. Infinite typical scale lengths (for finite wavelengths) are associated with periodic media for which it is known that no wave localization can occur due to perfect constructive and destructive interference, that is, certain frequencies are not attenuated at all, whereas others are immediately attenuated. However, the probability of a periodic layering (realization) occurring is zero.

3 NUMERICAL SIMULATIONS

3.1 Strategy and measurement method

To check to what degree theory and practice agree, numerical simulations must be performed. Therefore, with this aim in mind, measurements of $l(f)$, $Q^{-1}(f)$, $\delta c(f)$ and $\delta U(f)$ are made and compared with their theoretical predictions over a large range of $k_0'a$ and for media described by different autocorrelation functions. Although such comparisons have been made before, either measurements were averaged over a large number of realizations (Sheng *et al.* 1986) or only highly fluctuating estimates could be obtained (White *et al.* 1990; Shapiro *et al.* 1994; Shapiro & Hubral 1999), which are not as convincing as they could be. In this section, I present a method that is capable of producing accurate estimates of the desired quantities with only a limited number of fluctuations for a single realization of the medium by means of the wavelet transform.

In this paper, only the predictions of wave localization theory for a pulse that consists of plane waves and traverses a random medium has been described. As a consequence, only the transmission problem is dealt with in the numerical simulations. Hence, a source is placed in the homogeneous half-space beneath the random part of the medium and the first-arriving energy is recorded at the surface for two angles of incidence, namely 0° and 30°. This is done for four independent realizations each of three different autocorrelation functions with a typical scale length a of the heterogeneities of 10 m and relative standard deviations σ_κ of 15 and 30 per cent, respectively. Hence, a total of 24 simulations have been performed for two angles of incidence. The relative standard deviations of κ^{-1} correspond to relative standard deviations of, respectively, 7.5 and 15 per cent of the velocity for constant density. Table 1 displays the remaining constant parameters of the medium.

Table 1. Medium parameters. L: thickness of random layer; z_{source}: source depth; ρ_0: density; Δz: discrete layer thickness; Δt: sample time; $f_{\text{p,Ricker}}$: peak frequency of Ricker source wavelet.

L	4000 m	z_{source}	4000 m
c_0	4000 m s^{-1}	ρ_0	2.2 g cm^{-3}
Δz	1 m	Δt	1 ms
$f_{\text{p,Ricker}}$	150 Hz	a	10 m

Some additional remarks have to be made. An identical c_0 is used in both the random part of the medium and the matching half-space underneath it. No free surface is used to prevent back-scattering of energy from this interface. Finally, fluctuations are slightly damped at the edges to force all energy to enter the random medium. Moreover, a point source with a so-called Ricker source wavelet (second derivative of a Gaussian) is used instead of plane waves. Simulations are performed with an acoustic version of the method of Dietrich (1988) in which the generalized reflection and transmission matrix method of Kennett (1974) and the discrete wavenumber summation method of Bouchon (1981) have been combined.

The media with the required autocorrelation functions are created in the wavenumber domain. First, a random sequence is generated with a Gaussian distribution function and an autocorrelation function equaling a Dirac spike. Next, the sequence is transformed to the wavenumber domain, multiplied by the square root of the Fourier transform of the desired autocorrelation function and back-transformed to the space domain. The square root is needed to ensure that it is the autocorrelation function of the resulting sequence that has the desired form and not the created sequence itself.

Obviously, discrete representations of the desired media are employed as a finite layer thickness is used. Unfortunately, this means that perfectly smooth models and media displaying fluctuations on any scale cannot be handled well. Moreover, due to such finite layer thicknesses, variances are biased. The variances of discrete profiles should be inferior to their continuous counterparts (Frankel & Clayton 1986). Theoretical predictions are, therefore, slightly biased since this phenomenon is neglected in the numerical simulations and the profiles used.

To analyse the attenuation and dispersion of the primary (first arrival), traces are transformed to the frequency domain. However, this is done using not a Fourier transform but a wavelet transform. The inconvenience of the Fourier transform is that an optimal window length centred around the primary must be chosen, which may be problematic. On the one hand, results obtained by using long analysis windows are biased due to the presence of later-arriving energy. On the other hand, behaviour at low frequencies cannot be accurately measured using short window lengths. To circumvent this problem, use is made of a wavelet transform since it analyses the low-frequency content of data with long windows and the high frequencies with short ones. Hence, it forms a natural bridge between frequency and time analyses of non-stationary data.

The wavelet transform is most easily understood by drawing an analogy with the short-term Fourier transform, which is simply a repeated Fourier transform using a sliding window. It is expressed as

$$\mathscr{F}[s](f,\tau) = \int s(t) g^*(t-\tau)\, \mathrm{e}^{2\pi i f t} dt\,, \tag{52}$$

with $s(t)$ the recorded time signal and $g^*(t)$ the complex conjugate of the employed window $g(t)$, which has a fixed length. The continuous wavelet transform, on the other hand, is given by

$$\mathscr{W}[s](a_w,\tau) = a_w^{-1/2} \int s(t) w^*\left(\frac{t-\tau}{a_w}\right) dt\,, \tag{53}$$

where $w(.)$ represents the shifted and scaled mother wavelet and a_w denotes scale, which is inversely proportional to frequency. The normalization factor $a_w^{-1/2}$ ensures that wavelets have identical energy for any scale. The mother wavelet represents that type of wavelet used for signal analysis. A comparison of eqs (52) and (53) shows directly that in the wavelet transform, window length is not kept fixed, but displays the desired trade-off: it is dilated ($a_w > 1$) or contracted ($a_w < 1$) by changing the value of a_w. For more background, the interested reader is referred to the review papers of Rioul & Vetterli (1991) and Kumar & Foufoula-Georgiou (1997).

In this application, use will be made of the classical Morlet mother wavelet to analyse data. It is given by

$$w(t) = \frac{\pi^{1/4}}{c_w^{1/2}} \mathrm{e}^{-i\pi t'}\, \mathrm{e}^{\frac{1}{2}(\pi t'/c_w)^2} \tag{54}$$

(with $t' = t/\Delta t$). Hence, it is simply a real cosine plus complex sine weighted with a Gaussian with variance c_w/π to produce a local support. Expressing it in this form has the convenience that $a_w = 1$ equals the Nyquist frequency. Consequently, increasing a_w yields lower frequencies, i.e. $f = 1/(2\Delta t\, a_w)$. The constant c_w is set at 5.5 in this study.

To prevent source correction terms needing to be estimated to obtain accurate measurements of attenuation and dispersion, a totally homogeneous medium is used as a reference. Nevertheless, this medium has the same set-up as the other simulations, that is, the same number of layers, source and receiver positions, etc. Using such a reference has several advantages, namely, not only are source correction terms not needed, but in addition results are not biased by numerical dispersion. Moreover, no correction is required for spherical divergence either, thereby allowing for simulations with more complicated media.

The Appendix contains the exact measure method to estimate the localization length, the inverse quality factor and both the phase and group velocities.

3.2 Results

In the following, the numerical simulations are described and discussed. Fig. 2 shows an identical realization for the three types of autocorrelation functions used, namely Gaussian, exponential and Von Kármán for $\nu = 0$. It can be clearly seen that the Gaussian is the smoothest profile and this particular Von Kármán function the roughest one. The exponential function is somewhere in between these extremes. Moreover, although the typical scale length of the heterogeneities is 10 m, the profiles display clearly fluctuations on any scale length.

Fig. 3 displays parts of the resulting traces for the realization shown in Fig. 2 for two angles of incidence (0° and 30°) and two different values of σ_κ (15 and 30 per cent). Every second trace represents the case of $\phi_i = 30°$. The first two traces show the homogeneous case, the next six traces $\sigma_\kappa = 15$ per cent and the last six traces $\sigma_\kappa = 30$ per cent for Gaussian, exponential and Von Kármán media, respectively. Note that the last five traces are plotted on a different scale. No time-dependent amplitude corrections are applied.

Attenuation, phase distortions and dispersions of the primary purely due to scattering can be clearly detected by a simple comparison with the original source wavelet (as shown in the first two traces). The Gaussian correlation function for $\sigma_\kappa = 30$ per cent is a particularly interesting case as its primary for vertical incidence is only weakly attenuated (plotted on true scale), whereas the primary for $\phi_i = 30°$ is nearly completely

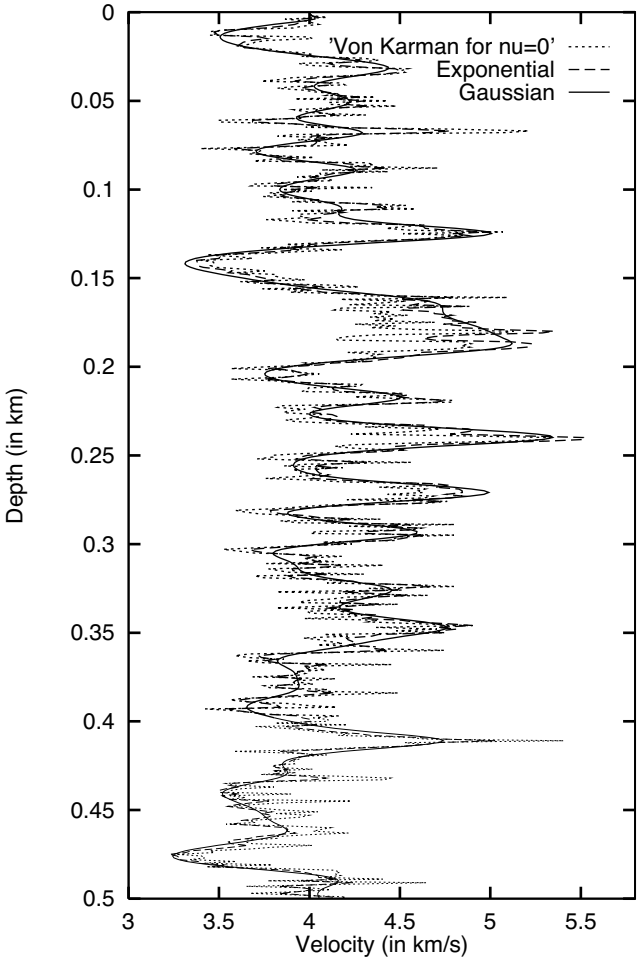

Figure 2. Top parts of the velocity profiles used for a single realization of Gaussian, exponential and Von Kármán ($\nu=0$) autocorrelation functions for $\sigma_\kappa=15$ per cent.

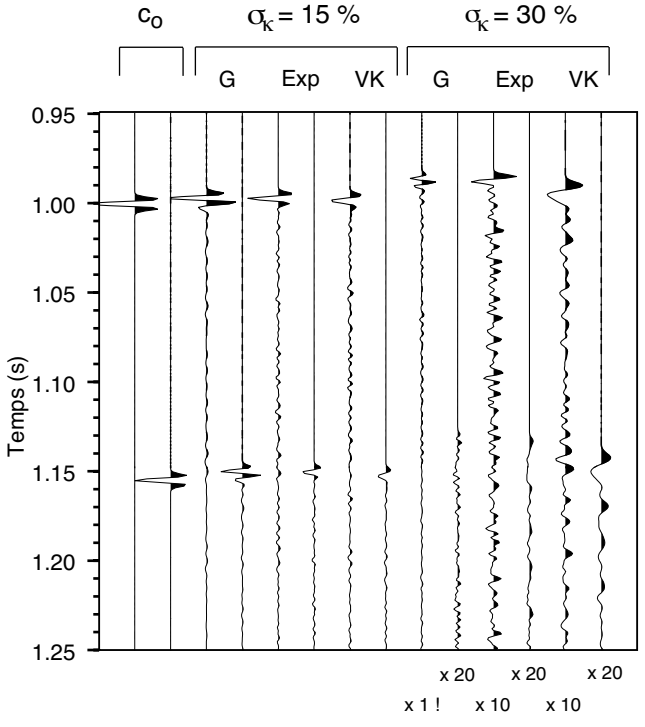

Figure 3. Primaries for the random media shown in Fig. 2. Every second trace shows the case of $\phi_i=30^\circ$. The first two traces display the homogeneous case, the next six traces $\sigma_\kappa=15$ per cent and the last six traces $\sigma_\kappa=30$ per cent. Notice different scale on last five traces. G stands for Gaussian, Exp for exponential and VK for Von Kármán autocorrelation functions.

attenuated (amplitudes multiplied by 20). This phenomenon is due to the strongly frequency- and angle-of-incidence-dependent attenuation factor for Gaussian media (see Fig. 1).

Fig. 4 displays the measured values for l, Q^{-1}, δc and δU for four different realizations each of the three types of autocorrelation functions used for both angles of incidence and a standard deviation of 15 per cent. Fig. 5 displays the same quantities for a standard deviation of 30 per cent of the fluctuations. Moreover, the theoretical predictions have been shown in both figures. Again, it should be noted that $\Gamma(0)$ used in the Von Kármán function has been replaced by a constant (13.0) chosen to display the general trend.

A close examination of Figs 4 and 5 reveals that theory and practice agree well, especially in the low to intermediate frequency range. For instance, l is proportional to f^{-2} at low frequencies and Q^{-1}, δc and δU all tend to zero in this limit, thereby confirming the existence of the homogenization phenomenon. In addition, δc and δU tend always to the geometric velocity in the high-frequency domain independent of the type of autocorrelation function used.

In the high-frequency domain, however, some discrepancies exist, although the general trend is confirmed. Most remarkable are discrepancies for $l(f)$ and δc as the localization length does not seem to display the e^{f^2} dependence for Gaussian media and all theoretical predictions are systematically too low for δc. Due to the blocky character of the measurements of δU, it cannot be concluded if the theoretical predictions of δU in the high frequency have also been underestimated. Nevertheless, it should be noted that part of such discrepancies are due to the fact that a finite layer thickness has been used as discussed above. Hence, profiles are not smooth and theoretical variances may have been underestimated.

Finally, it should be noted that few fluctuations exist in the estimates of the various quantities and that they seem to diminish with frequency (in particular for δc and l, the self-averaging quantities). Estimates of Q^{-1} and δU are more strongly fluctuating than those for l and δc as these are not self-averaging quantities.

4 DISCUSSION

Before relating the obtained results to other known results, I discuss self-averaging and its implications as it is one of the most important features of the theory described above. Self-averaging of certain quantities allows for the application of a statistical approach to the wave scattering problem, thereby significantly simplifying the mathematics while at the same time producing real observables that can be measured and e.g. inverted for. The main characteristic of self-averaging variables is that they display a Gaussian distribution centred around their expected values, at least in some macroscopic limit (Gredeskul & Freĭlikher 1990). Moreover, the variance of the self-averaging quantity is inversely proportional to the thickness of the chaotic medium for 1-D systems. Thus, in the limit of an infinitely thick medium, the variance will reduce to zero, resulting in a

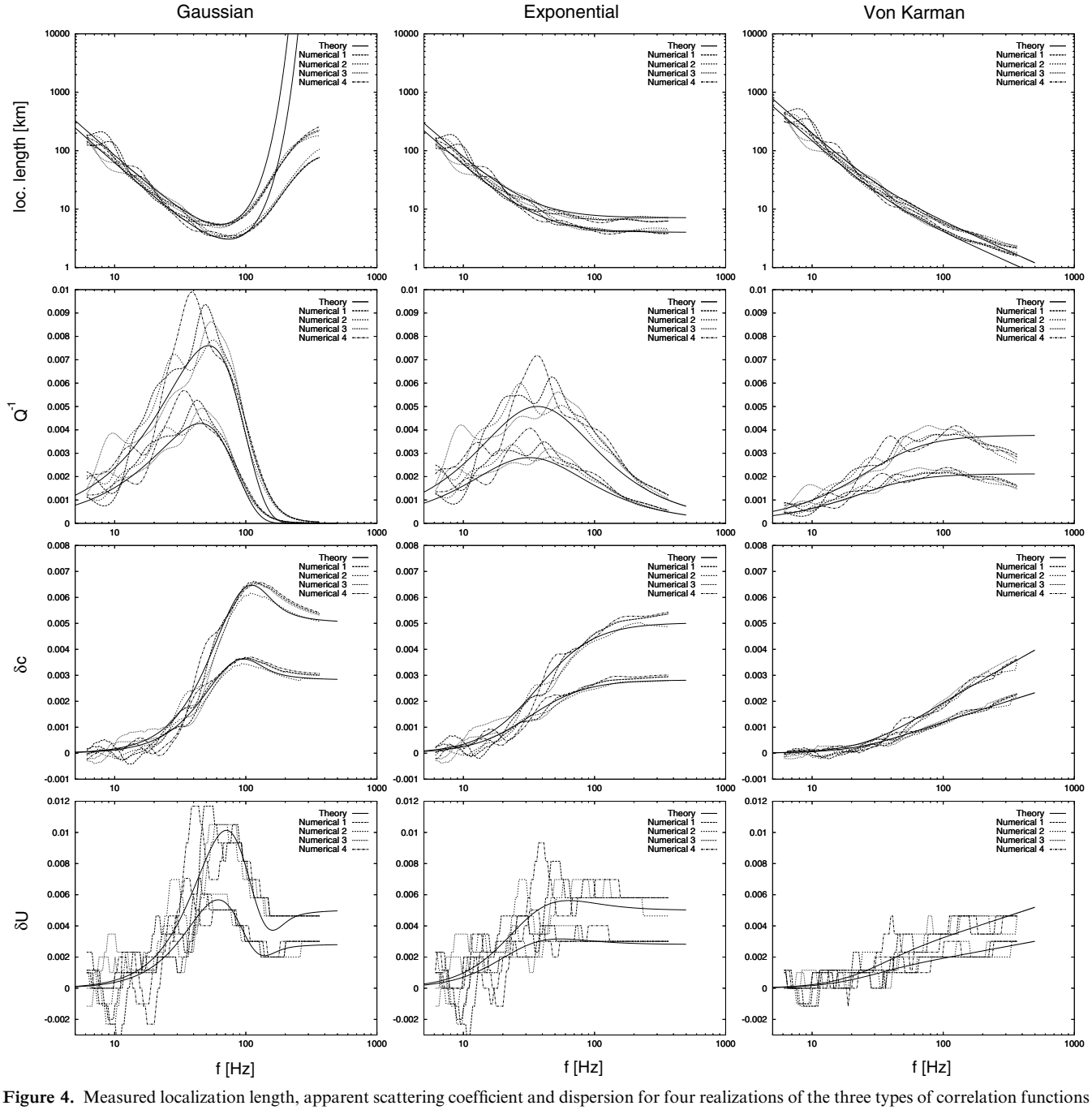

Figure 4. Measured localization length, apparent scattering coefficient and dispersion for four realizations of the three types of correlation functions used for both angles of incidence for $\sigma_\kappa = 15$ per cent. Theoretical predictions are also plotted. The lowest theoretical curve is for $\phi_i = 0$ and the other $\phi_i = 30^\circ$ except in the first row. The blocky character of δU is due to the sampling rate used (1 ms). Note, however, that the values of δc have been calculated with a precision higher than the sampling rate.

probability distribution resembling a Dirac positioned at the expected value. That is, the expected value has unit probability in this limit for (almost) any realization of the medium, which is the strict requirement for self-averaging. Finally, it should be noted that convergence of self-averaging quantities is assumed to be fast, once the thickness of the random medium exceeds the localization length (Souillard 1987; Van Tiggelen 1999).

As can be seen in Figs 4 and 5, fluctuations of the localization length and the relative velocity dispersion are decreasing with increasing frequency. Two features contribute to this phenomenon. First, a Ricker wavelet has been used with a peak frequency of 150 Hz and a limited bandwidth. Such a source wavelet is not very energetic at low frequencies, thereby rendering an exact validation more difficult. On the other hand, fluctuations are nearly absent for high frequencies, while the source wavelet does not contain many high frequencies either. Second, fluctuations of self-averaging quantities should increase if kL diminishes (fewer cycles), which is the case for decreasing frequencies.

Using a wavelet transform for signal analysis has tremendously reduced fluctuations, as can be concluded from a comparison with the results of e.g. Sheng *et al.* (1986), White *et al.* (1990),

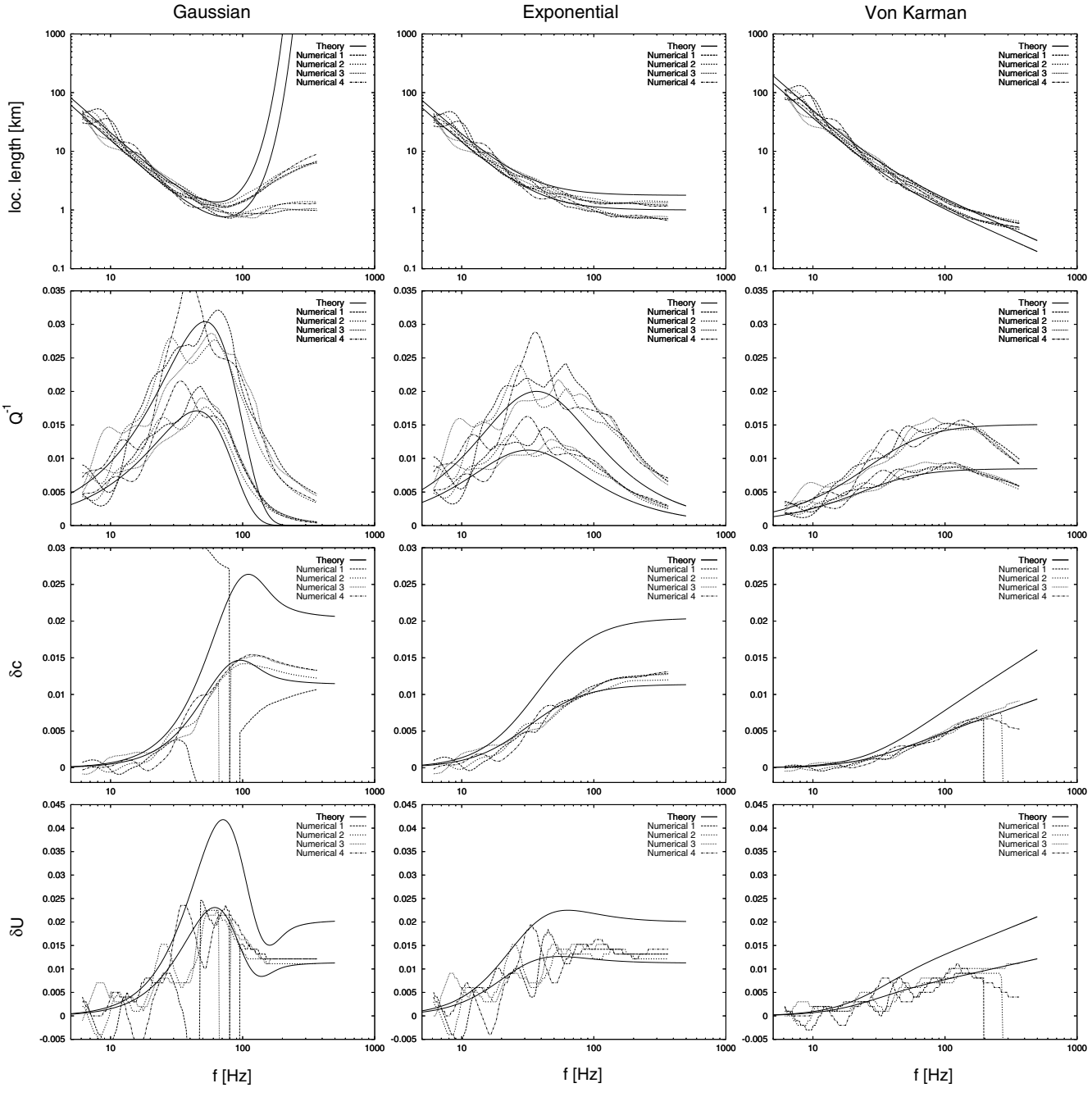

Figure 5. Identical to Fig. 4 for $\sigma_\kappa = 30$ per cent. Group and phase velocity measurements have not been displayed for $\phi_i = 30^\circ$ as phase unwrapping became completely unstable and the primary could not be automatically detected (main energy arrived after the primary). Notice changed vertical scales with respect to Fig. 4.

Shapiro *et al.* (1994) and Shapiro & Hubral (1999). These reduced fluctuations are probably due to two characteristics of the wavelet transform. First, it uses an optimal analysis window length for each frequency considered since later-arriving energy produces a minimal distortion of results and energy of low frequencies is not underestimated due to window lengths that are too short. Second, the estimation quality of self-averaging quantities can be increased by averaging over some other variable over a mesoscopic length scale such as, for example, the pulse length (Gredeskul & Freĭlikher 1990). As the wavelet transform analyses data over several periods, such an averaging is explicitly applied, thereby increasing the quality of the estimates. Interestingly, the wavelet transform was conceived by Morlet *et al.* (1982) in the context of sampling theory and wave scattering, albeit due to periodic layering.

Therefore, the use of the wavelet transform has allowed us to obtain clear indications of the validity range of the developed theory. Theory and numerical simulations closely agree up to 100 Hz for both angles of incidence and the three types of autocorrelation functions considered, i.e. $k_0'a \approx 1.5$ and $k_0 L \approx 600$. Minor discrepancies can be seen above this value. Two reasons may explain these deviations. First, the above-described multiple scattering theory of Shapiro & Zien (1993) is a second-order theory. Hence, results may become less accurate

for large perturbations of parameters. Second, numerical simulations have been performed using discrete profiles with exactly the desired standard deviations. However, discrete sequences should have standard deviations slightly inferior to their continuous equivalents. Hence, theoretical standard deviations may have been underestimated. Indeed, slightly increasing the theoretical σ_κ does diminish the existing gaps, but is not able to explain all deviations.

Nevertheless, the validity range covers most interesting frequencies and wavelengths. For instance, theory is accurate in the domain of Mie scattering, where wavelengths and typical scale lengths of heterogeneities are comparable. Therefore, theoretical predictions of the localization length hold true in a much broader frequency range than those published by Burridge *et al.* (1994) and Clouet & Fouque (1994), which are only valid in the low-frequency domain (Rayleigh scattering). In addition, expressions are given for determining directly the frequency-dependent dispersion. Nevertheless, predictions should coincide in the low-frequency domain.

In this paper, wave localization has been primarily presented to increase our understanding of strong multiple wave scattering. However, to reduce mathematical complications and to emphasize some implications for multiple scattering of waves, several simplifications have been made and the theory has been described in its simplest form. On the other hand, the full range of implications of wave localization is not yet known. In particular, the question whether wave localization occurs in real 3-D media is unresolved, although experiments of Wiersma *et al.* (1997) with light do point in this direction. Van der Baan (1999) discussed briefly some of the other complications such as the influence of elasticity, non-stationary fluctuations, non-perfect layering and wave localization in higher dimensions. Nevertheless, two mathematical simplifications can easily be dropped.

First, in Shapiro *et al.* (1994) equations are obtained for the localization length and the vertical phase velocity for random density profiles. Fluctuations in density increase the apparent attenuation due to scattering because of increased impedance contrasts. However, as it is often assumed that velocity and density fluctuations are correlated in the real Earth (see e.g. Sato & Fehler 1998), it might be interesting to express the self-averaging quantities directly in terms of impedance fluctuations instead of velocity, compressibility and density fluctuations.

Second, dissipation of energy or intrinsic attenuation is often thought to exist independently of apparent attenuation due to scattering (Herraiz & Espinosa 1987; Beltzer 1988). This implies that besides the Lyapunov exponent, γ_{sc}, for attenuation due to wave scattering, a second 'Lyapunov exponent', γ_{in}, for intrinsic scattering can be introduced, and that the 'total Lyapunov exponent', γ_{tot}, is given by a simple summation of γ_{sc} and γ_{in}, thereby again increasing attenuation.

5 CONCLUSIONS

Multiple wave scattering is a complex phenomenon. Using a statistical description of the chaotic part of the medium reduces the mathematics involved considerably. However, such an approach usually does not result in real observables unless self-averaging quantities are considered.

Wave localization permits such a statistical approach and produces, in addition, two self-averaging quantities, namely the Lyapunov exponent and the effective vertical wavenumber. The frequency-dependent localization length, i.e., the penetration depth, the inverse quality factor and the dispersion (phase and group velocities) all purely due to wave scattering can be calculated with these two observables. These variables have been calculated using the second-order perturbation expansion of Shapiro & Zien (1993) for several chaotic media described by different autocorrelation functions. Media used range from very smooth to fractal-like.

Analysis of the results shows that the localization length is always proportional to f^{-2} in the low-frequency domain independent of the type of medium. This is characteristic for Rayleigh scattering in 1-D media. In the high-frequency domain, it either diverges or converges to zero. The localization length only approaches a constant for exponential autocorrelation functions associated with piecewise continuous models. Hence, minimal localization lengths as inferred by Sheng *et al.* (1986) do not necessarily exist for very rough and fractal-like media.

Moreover, it is confirmed that waves always become localized in 1-D media if a small amount of randomness is present, save for a countable number of exceptions. These exceptions include the long-wavelength limit in which the medium becomes effectively homogeneous as implied by effective medium theory and in smooth media in the short-wavelength or geometric limit in which no heterogeneities (discontinuities) exist either.

Inspection of the inverse quality factor indicated that Mie scattering yields the most effective apparent attenuation due to scattering. On the other hand, fractal-like media form an exception as the reciprocal of the quality factor rises monotonically with frequency and approaches a constant, making it effectively constant over a large range of frequencies. Therefore, no particular ratio ka is favoured for such media.

The last quantity that has been examined is the frequency-dependent dispersion due to scattering. It has been shown that predictions of wave localization theory for the apparent attenuation and the phase velocities are consistent with the Kramers–Krönig relations. Therefore, the theory respects causality. Moreover, it is confirmed that anisotropy exists due to the existence of fine-scale layering.

Both the phase and group velocities always converge, independent of the type of medium, to the same limits for both high and low frequencies. That is, they approach the effective medium velocity in the long-wavelength limit and the geometric velocity in the high-frequency limit. However, for intermediate frequencies, large differences occur. For instance, unlike rough media where the phase velocity is monotonically rising with frequency, in smooth media an overshoot occurs. This implies that the geometric velocity is not the highest encountered phase velocity, but an intermediate range of frequencies exist that arrive before the highest frequencies in smooth models. This particular phenomenon occurs to prevent causality being violated. In addition, the exact shape of the group velocity curves and the number of Airy phases also strongly depend on the type of autocorrelation function. Moreover, Airy phases often occur in the domain of Mie scattering. Hence, they cannot always be associated with strong arrivals, contrary to the common assumption.

Finally, numerical simulations have clearly confirmed the theoretical predictions as theory and practice coincide for values of ka up to 1.5, thereby including both Rayleigh and Mie scattering, and for very large propagation distances, i.e. $kL \approx 600$. In addition, above this value, the general trend is affirmed. Discrepancies for the higher frequencies are probably

due to the use of discretized models for the numerical simulations and the fact that a second-order theory has been applied. In contrast to previous simulations, highly accurate estimates of all parameters could be made by means of the wavelet transform, which damped out nearly all perturbing fluctuations.

ACKNOWLEDGMENTS

I would like to thank Michel Bouchon for discussions concerning the implications of the theoretical predictions and Michel Dietrich for providing his numerical code. Moreover, I am indebted to Sergei Shapiro, who was always willing to discuss and explain details of his theoretical development and wave localization theory in general. Finally, the original manuscript benefited from comments and suggestions made by the editor and an anonymous reviewer.

REFERENCES

Abrahams, E., Anderson, P.W., Licciardello, D.C. & Ramakrishnan, T.V., 1979. Scaling theory of localization: absence of quantum diffusion in two dimensions, *Phys. Rev. Lett.,* **42,** 673–676.

Abramowitz, M. & Stegun, I.A., 1972. *Handbook of Mathematical Functions,* Dover Publications, New York.

Anderson, P.W., 1958. Absence of diffusion in certain random lattices, *Phys. Rev.,* **109,** 1492–1505.

Asch, M., Kohler, W., Papanicolaou, G., Postel, M. & White, B., 1991. Frequency content of randomly scattered signals, *SIAM Rev.,* **33,** 526–629.

Backus, G.E., 1962. Long-wave elastic anisotropy produced by horizontal layering, *J. geophys. Res.,* **67,** 4427–4440.

Beltzer, A.I., 1988. Dispersion of seismic waves by a causal approach, *Pure appl. Geophys.,* **128,** 147–156.

Bouchon, M., 1981. A simple method to calculate Green's functions for elastic layered media, *Bull. seism. Soc. Am.,* **71,** 959–971.

Burridge, R., Lewicki, P. & Papanicolaou, G., 1994. Pulse stabilization in a strongly heterogeneous medium, *Wave Motion,* **20,** 177–195.

Clouet, J.F. & Fouque, J.P., 1994. Spreading of a pulse traveling in random media, *Ann. appl. Probability,* **4,** 1083–1097.

Delyon, F., Kunz, H. & Souillard, B., 1983. 1D wave equations in disordered media, *J. Phys. A,* **16,** 25.

Dietrich, M., 1988. Modeling of marine seismic profiles in the $t-x$ and $\tau-p$ domains, *Geophysics,* **53,** 453–465.

Dorren, H.J.S. & Snieder, R.K., 1995. The stability of finite-dimensional inverse problems, *Inverse Problems,* **11,** 889–911.

Frankel, A. & Clayton, R.W., 1986. Finite difference simulations of seismic scattering: implications for the propagation of short-period seismic waves in the crust and models of crustal heterogeneity, *J. geophys. Res.,* **91,** 6465–6489.

Frisch, U., 1968. Wave propagation in random media, in *Probabilistic Methods in Applied Mathematics,* pp. 75–198, ed. Bharucha-Reid, A.T., Academic Press, San Diego.

Fürstenberg, H., 1963. Noncommuting random products, *Trans. Am. Math. Soc.,* **108,** 377.

Gradshteyn, I.S. & Ryzhik, I.M., 1980. *Table of Integrals, Series and Products,* Academic Press, San Diego.

Gredeskul, S.A. & Freĭlikher, V.D., 1990. Localization and wave propagation in randomly layered media, *Soviet Phys. Uspekhi,* **33,** 134–146.

Herraiz, M. & Espinosa, A.F., 1987. Coda waves: a review, *Pure appl. Geophys.,* **125,** 499–577.

Kennett, B.L.N., 1974. Reflections, rays and reverberations, *Bull. seism. Soc. Am.,* **64,** 1685–1696.

Kumar, P. & Foufoula-Georgiou, E., 1997. Wavelet analysis for geophysical applications, *Rev. Geophys.,* **35,** 385–412.

Lifshits, I., Gredeskul, S.A. & Pastur, L., 1988. *Introduction to the Theory of Disordered Systems,* John Wiley, New York.

Morlet, J., Arens, G., Fourgeau, E. & Giardt, D., 1982. Wave propagation and sampling theory—Part II: Sampling theory and complex waves, *Geophysics,* **47,** 222–236.

Oseledec, V., 1968. A multiplicative ergodic theorem. Lyapunov characteristic numbers for dynamical systems, *Trans. Moscow Math. Soc.,* **19,** 197–231.

Ramakrishnan, T.V., 1987. Electron localization, in *Chance and Matter,* pp. 213–304, eds Souletie, J., Vannimenus, J. & Stora, R., Elsevier, Amsterdam.

Rioul, O. & Vetterli, M., 1991. Wavelets and signal processing, *IEEE Sign. Process. Mag.,* **8,** 14–38.

Sato, H. & Fehler, M., 1998. *Seismic Wave Propagation and Scattering in the Heterogeneous Earth,* Springer-Verlag, New York.

Scales, J.A., 1993. On the use of localization theory to characterize elastic wave propagation in randomly stratified 1-D media, *Geophysics,* **58,** 177–179.

Shapiro, S.A. & Hubral, P., 1999. Elastic waves in random media—fundamentals of seismic stratigraphic filtering, *Lecture Notes in Earth Sciences,* Vol. 80, Springer Verlag, Berlin.

Shapiro, S.A. & Zien, H., 1993. The O'Doherty-Anstey formula and the localization of seismic waves, *Geophysics,* **58,** 736–740.

Shapiro, S.A., Zien, H. & Hubral, P., 1994. A generalized O'Doherty-Anstey formula for waves in finely layered media, *Geophysics,* **59,** 1750–1762.

Sheng, P., 1995. *Introduction to Wave Scattering, Localization and Mesoscopic Phenomena,* World Scientific, Singapore.

Sheng, P., White, B., Zhang, Z.-Q. & Papanicolaou, G., 1986. Minimum wave-localization length in a one-dimensional random medium, *Phys. Rev. B,* **34,** 4757–4761.

Snieder, R., 1990. *Linearized Inversion of Seismic Waveforms,* Lecture Notes, University of Utrecht.

Souillard, B., 1987. Waves and electrons in inhomogeneous media, in *Chance and Matter,* pp. 305–381, eds Souletie, J., Vannimenus, J. & Stora, R., North-Holland, Elsevier, Amsterdam.

Tatarskii, V.I., 1961. *Wave Propagation in a Turbulent Medium,* McGraw-Hill, New York.

Van der Baan, M., 1999. Deux méthodes d'inférence statistique appliquées aux données de sismique réflexion profonde: détection de signaux et localisation d'onde, *PhD thesis,* University Joseph Fourier, Grenoble.

Van Tiggelen, B.A., 1999. Localization of waves, in *Diffuse Waves in Complex Media,* pp. 1–60, ed. Fouque, J.P., Kluwer Academic, Dordrecht.

Virster, A.D., 1979. On the products of random matrices and operators, *Theor. Prob. Appl.,* **24,** 367.

White, B., Sheng, P. & Nair, B., 1990. Localization and backscattering spectrum of seismic waves in stratified lithology, *Geophysics,* **55,** 1158–1165.

Wiersma, D.S., Bartolini, P., Lagendijk, A. & Righini, R., 1997. Localization of light in a disordered medium, *Nature,* **390,** 671–673.

APPENDIX A: MEASUREMENT METHOD

Like any complex number, $\mathcal{W}[s](a_w, \tau)$ can be expressed in the polar form $r(a_w, \tau)\exp\{i\theta(a_w, \tau)\}$, where r depends on the source wavelet, its radiation pattern and attenuation, and θ on the initial phase of the source wavelet and dispersion.

Determination of the desired frequency-dependent apparent attenuation and dispersion is straightforward. Let $r_i^{\max}(a_w, \tau_i^{\max})$ denote the maximum amplitude of the wavelet coefficients for a given a_w or frequency measured at time $\tau_i^{\max}$. In general, $r_i^{\max}$ represents the peak amplitude of the primary for a specific frequency and $\tau_i^{\max}$ its arrival time, unless scattering has become

too strong, that is, the main energy arrives after the primary. Moreover, let $i=1$ define a realization of some heterogeneous model and $i=0$ the homogeneous case. The localization length can now be estimated using eq. (13) with $|T|=r_1^{\max}/r_0^{\max}$ and $z=L/\cos(\phi_i)$, i.e.

$$l(a_w)=\frac{-L}{\cos(\phi_i)\ln(r_1^{\max}/r_0^{\max})}\,. \tag{A1}$$

In addition, Q^{-1} is calculated using expression (19).

The dispersion δc is obtained in a similar way using the difference of the arguments $\theta_1^{\max}$ and $\theta_0^{\max}$, which should equal

$$\delta\theta=\theta_1^{\max}-\theta_0^{\max}=(k_{z,1}-k_{z,0})L-\omega(\tau_1^{\max}-\tau_0^{\max})\,. \tag{A2}$$

The horizontal wavenumber is not involved as it was assumed to be constant. Moreover, since the vertical wavenumber k_z equals ψ, the previous expression yields

$$\delta c=\frac{-s_c}{1+s_c},\quad\text{with}\quad s_c=\frac{c_0\left[\delta\theta+\omega(\tau_1^{\max}-\tau_0^{\max})\right]}{\omega L\cos(\phi_i)} \tag{A3}$$

using eq. (20). Finally, it should be noted that $\delta\theta$ represents the unwrapped phase. Phase unwrapping is best done starting at the lowest frequencies, i.e. high values of a_w.

The corresponding equation for δU is found by putting

$$\frac{\partial\delta\theta}{\partial\omega}=0\,, \tag{A4}$$

yielding

$$\delta U=\frac{-s_u}{1+s_u}\quad\text{with}\quad s_u=\frac{(\tau_1^{\max}-\tau_0^{\max})c_0}{L\cos(\phi_i)} \tag{A5}$$

using eqs (A2) and (21).